JOURNAL OF GUIDANCE, CONTROL, AND DYNAMICS
Vol. 28, No. 1, January–February 2005

Reduced Hamiltonian Dynamics for a Rigid Body/Mass Particle System

Craig A. Woolsey*
Virginia Polytechnic Institute and State University, Blacksburg, Virginia 24061-0203

Three equivalent reduced-dimensional Hamiltonian systems that model a rigid body in a perfect fluid coupled to a moving-mass particle are presented. These Hamiltonian systems describe the dynamics of an underwater vehicle with a moving-mass actuator or a flexible internal appendage. The systems include, as a special case, models for a spacecraft coupled to a moving mass. The Hamiltonian models are noncanonical; the structure of Hamilton's equations is defined by the Poisson tensor, a generalization of the symplectic matrix from classical mechanics. The three models presented trade complexity of the generalized inertia tensor for complexity of the Poisson tensor. One model has a highly coupled inertia tensor and a block-diagonal Poisson tensor, whereas another has a highly coupled Poisson tensor and a block-diagonal inertia tensor. Two cases are considered. The first is that of an unconstrained mass particle. The second is that of a mass particle constrained to move in a linear track. Examples are included to illustrate the use of these models for nonlinear stability analysis.

Nomenclature

$\boldsymbol{b}_i$	=	ith basis vector for body frame
$\boldsymbol{C}_f$	=	hydrodynamic coupling matrix
C_i	=	Casimir function
$\boldsymbol{e}_i$	=	ith basis vector for $\mathbb{R}^3$
$\boldsymbol{G}$	=	input matrix
g	=	acceleration caused by gravity
$\boldsymbol{H}$	=	angular momentum about inertial origin
$\mathcal{H}$	=	Hamiltonian
$\boldsymbol{h}$	=	angular momentum about body origin
$\mathbb{I}$	=	generalized inertia
$\boldsymbol{I}_i$	=	ith basis vector for inertial frame
$\boldsymbol{J}_b$	=	rigid-body inertia
$\boldsymbol{J}_f$	=	added inertia
$\boldsymbol{M}_f$	=	added mass (a matrix)
m	=	mass of displaced fluid
m_b	=	mass of body
m_p	=	mass of particle
$\boldsymbol{P}$	=	inertial linear momentum (inertial frame)
$\boldsymbol{p}$	=	inertial linear momentum (body frame)
$\boldsymbol{\mathcal{R}}$	=	body to inertial rotation
$\boldsymbol{R}_p$	=	relative particle position (inertial frame)
$\boldsymbol{r}_{cg}$	=	body center of gravity
$\boldsymbol{r}_p$	=	relative particle position (body frame)
r_{p_1}	=	$\boldsymbol{e}_1 \cdot \boldsymbol{r}_p$
T	=	kinetic energy
U	=	potential function
$\boldsymbol{u}$	=	input; force applied to particle by body
$\boldsymbol{v}$	=	body translational velocity (body frame)
$\boldsymbol{v}_p$	=	inertial velocity of particle (body frame)
v_{p_1}	=	$\boldsymbol{e}_1 \cdot \boldsymbol{v}_p$
$\tilde{\boldsymbol{v}}_p$	=	$\boldsymbol{v}_p - \boldsymbol{v}$
$\tilde{v}_{p_1}$	=	$\boldsymbol{e}_1 \cdot \tilde{\boldsymbol{v}}_p$
$\boldsymbol{X}$	=	inertial position of body origin
$\boldsymbol{X}_p$	=	inertial position of particle
$\boldsymbol{z}$	=	state vector for a Hamiltonian system
$\boldsymbol{\gamma}$	=	$\boldsymbol{\mathcal{R}}^T \boldsymbol{I}_3$; direction of gravity (body frame)
$\boldsymbol{\eta}$	=	generalized velocity
$\boldsymbol{\Lambda}$	=	Poisson tensor
$\boldsymbol{\nu}$	=	generalized momentum
$\boldsymbol{\omega}$	=	body angular velocity (body frame)
$\boldsymbol{0}$	=	column vector of three zeros
$\mathbb{0}$	=	3×3 matrix of zeros
$\mathbb{1}$	=	3×3 identity matrix
$\mathbb{1}_{23}$	=	$\mathbb{1} - \boldsymbol{e}_1 \boldsymbol{e}_1^T$
$\nabla()$	=	gradient of a function (treated as a column vector)

Subscripts

b	=	rigid body
b/f	=	rigid body/fluid system
b/p	=	rigid-body/mass particle system
f	=	fluid
p	=	mass particle
sys	=	rigid-body/fluid/mass particle system

I. Introduction

INTERNAL degrees of freedom can influence a vehicle's dynamics, either adversely or advantageously, in complicated ways. Simple models for the coupled dynamics can provide insight into the system's behavior. For example, a model for an aircraft with a mass particle oscillator has been used to show that fuel slosh can excite undesired lateral-directional dynamics.[1] Similarly, a mass particle model for oscillating fuel slag in a solid rocket engine has provided a plausible explanation for a coning instability observed in some orbit transfer boosters.[2] Damped point-mass oscillators serve as precession or nutation dampers in gyrostats, an application that leads to some intriguing problems in dynamical systems theory.[3,4]

Internal moving elements can also provide actuation. Internal actuators offer advantages over conventional actuators that make them appealing in many vehicle applications. In space applications, internal actuators are useful because they can be powered using readily generated electricity rather than costly propellant. For example, moving-mass actuators have recently been proposed as a cost-effective means for precision orbit regulation for spacecraft flying in formation.[5] Prismatic actuators intended for other uses, such as deploying solar arrays, can also be used to effect maneuvers as described in Ref. 6. Internal actuators are appealing for atmospheric reentry vehicles because they are impervious to the high temperatures and forces of hypersonic reentry.[7,8] For underwater vehicles, internal actuators are appealing because they can be used at low velocity, where fins lose control authority.[9] Moreover, because they are housed within the hull they are not susceptible to corrosion and biological fouling, which can incapacitate external

Received 23 September 2003; revision received 16 August 2004; accepted for publication 2 September 2004.

*Assistant Professor, Aerospace and Ocean Engineering; cwoolsey@vt.edu.

actuators. One intriguing application for moving-mass control in underwater vehicles is the underwater glider, a winged underwater vehicle that propels itself by alternately adjusting its center of mass and its net weight.[10]

This paper develops three reduced-dimensional Hamiltonian models for a rigid-body interacting with a moving-mass particle in a perfect fluid. Two cases are considered: a mass particle whose motion is unconstrained and a mass particle that is confined to move along a linear track. Reduction is possible because of symmetry in the dynamic equations. This symmetry corresponds to arbitrary translations of the inertial frame and rotations about the direction of gravity. Although these models are presented with an eye toward underwater vehicle applications, they are also relevant for space and atmospheric applications.

The force of interaction between the body and mass particle is treated as an input, although this "control force" can generally be interpreted as any force of interaction. In the absence of external forces and moments, the total energy is conserved. Moreover, because the control force is internal, total momentum is conserved for any choice of control. These observations are useful for control design and in studying stability of steady motions.

Each mathematical model presented here takes the form of an underactuated, noncanonical Hamiltonian control system. Suppose the state of a certain system is described by the state vector z. If the system is Hamiltonian, its dynamics can be expressed in terms of a bilinear, skew-symmetric operation known as the Poisson bracket $\{\cdot,\cdot\}$. This operation takes smooth functions $F(z)$ and $G(z)$ and generates a new smooth function according to the relation

$$\{F(z), G(z)\} = \nabla F^T \boldsymbol{\Lambda}(z) \nabla G$$

The skew-symmetric Poisson tensor $\boldsymbol{\Lambda}$ defines the structure of Hamilton's equations. For a canonical Hamiltonian system, in which z is the vector of generalized coordinates and conjugate momenta, the Poisson tensor corresponds to the matrix $\boldsymbol{J}$ in symplectic notation.[11]

Let $\mathcal{H}(z)$ be the Hamiltonian. Then the rate of change of any smooth function $F(z)$ is $\dot{F} = \{F, \mathcal{H}\}$. In particular, we have $\dot{z}_i = \{z_i, \mathcal{H}\}$, where z_i is the ith component of z. Alternatively, one can write

$$\dot{z} = \boldsymbol{\Lambda}(z)\nabla\mathcal{H}(z)$$

Note that $\dot{\mathcal{H}} = \{\mathcal{H}, \mathcal{H}\} = 0$ by skew symmetry of $\boldsymbol{\Lambda}$, confirming that the Hamiltonian is conserved. Moreover, any smooth function $C(z)$ whose gradient lies in the null space of $\boldsymbol{\Lambda}$ is conserved because this implies that $\{C, \mathcal{H}\} = 0$. Such a function is called a Casimir. Two Casimirs are called independent if their gradients are linearly independent. Conserved quantities, such as the Hamiltonian and Casimir functions, are useful in studying stability of steady vehicle motions. See Ref. 12 for a thorough discussion.

The general form of a noncanonical Hamiltonian control system is

$$\dot{z} = \boldsymbol{\Lambda}(z)\nabla\mathcal{H}(z) + \boldsymbol{G}(z)\boldsymbol{u} \tag{1}$$

where $\boldsymbol{u}$ denotes a vector of control inputs depending on time and possibly the state z. Hamiltonian control systems exhibit structure, which can be exploited for stability analysis and control design. Special tools for stability analysis include formal methods for constructing Lyapunov functions, such as the energy-Casimir method.[12] Such techniques are valuable because nonlinear stability of Hamiltonian systems cannot generally be determined through spectral analysis. Special tools for nonlinear control design include algorithms that shape the total energy and the dynamic structure represented by the Poisson tensor.[13,14]

A general transformation theory for noncanonical Hamiltonian control systems is presented in Ref. 15; however, the theory provides little guidance for choosing the actual transformation. In this paper, the various models reflect physically meaningful choices in the representation of kinetic energy. The Hamiltonian models presented here trade complexity of the Hamiltonian for complexity of the Poisson tensor. This tradeoff can make one particular model more or less useful than another for a given application. Indeed, as illustrated in Ref. 15, having alternative Hamiltonian representations available can greatly simplify nonlinear control design and stability analysis.

The paper is organized as follows. Section II describes the case where the mass particle is unconstrained. Three reduced Hamiltonian models are presented corresponding to three views of the system state. Section II ends with an example involving stability of steady translation of a streamlined underwater vehicle. In Sec. III, the special case of a mass particle constrained to a linear track is considered. Again, three models are presented. These correspond, to some extent, with those presented in Sec. II; however, the results presented in Sec. III are not a trivial special case. Section III ends with an example involving stability of steady major axis rotation of a spacecraft with a spring-mass oscillator. Section IV provides some concluding remarks.

II. Unconstrained Mass Particle

Figure 1 depicts a rigid body and a mass particle immersed in an ideal fluid. A reference frame with orthonormal basis $(\boldsymbol{I}_1, \boldsymbol{I}_2, \boldsymbol{I}_3)$ is fixed in inertial space. Another reference frame with orthonormal basis $(\boldsymbol{b}_1, \boldsymbol{b}_2, \boldsymbol{b}_3)$ is fixed in the body. The proper rotation matrix $\boldsymbol{\mathcal{R}}$ transforms free vectors from the body reference frame to the inertial reference frame. The inertial vectors $\boldsymbol{X}$ and $\boldsymbol{X}_p$ locate the origin of the body frame and the mass particle, respectively, in inertial space. Throughout the paper, lowercase boldfaced characters will represent vectors expressed in the body frame. Uppercase boldfaced characters will represent vectors expressed in the inertial frame. Exceptions, such as the rotation matrix $\boldsymbol{\mathcal{R}}$, will be clear from context.

A. Kinematics

Let the body frame vectors $\boldsymbol{\omega}$ and $\boldsymbol{v}$ represent, respectively, the angular and linear velocity of the body with respect to inertial space. Define the operator $\hat{}$ by requiring that $\hat{\boldsymbol{a}}\boldsymbol{b} = \boldsymbol{a} \times \boldsymbol{b}$ for vectors $\boldsymbol{a}, \boldsymbol{b} \in \mathbb{R}^3$. In matrix form,

$$\hat{\boldsymbol{a}} = \begin{pmatrix} 0 & -a_3 & a_2 \\ a_3 & 0 & -a_1 \\ -a_2 & a_1 & 0 \end{pmatrix}$$

The kinematic equations for the body are

$$\dot{\boldsymbol{\mathcal{R}}} = \boldsymbol{\mathcal{R}}\hat{\boldsymbol{\omega}} \tag{2}$$

$$\dot{\boldsymbol{X}} = \boldsymbol{\mathcal{R}}\boldsymbol{v} \tag{3}$$

Let the body vector $\boldsymbol{v}_p$ denote the velocity of the mass particle with respect to inertial space. The kinematic equation for the mass particle is

$$\dot{\boldsymbol{X}}_p = \boldsymbol{\mathcal{R}}\boldsymbol{v}_p \tag{4}$$

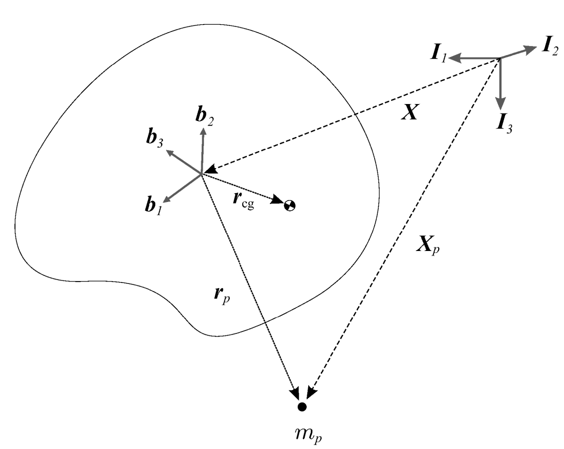

Fig. 1 Rigid body and mass particle in a fluid.

Now let the inertial vector $\boldsymbol{R}_p = \boldsymbol{X}_p - \boldsymbol{X}$ denote the position of the mass particle relative to the origin of the body frame. Define the body vector $\tilde{\boldsymbol{v}}_p = \boldsymbol{v}_p - \boldsymbol{v}$. An alternative kinematic equation for the mass particle is

$$\dot{\boldsymbol{R}}_p = \mathcal{R}\tilde{\boldsymbol{v}}_p \tag{5}$$

Finally, define $\boldsymbol{r}_p = \mathcal{R}^T \boldsymbol{R}_p$ to be the vector $\boldsymbol{R}_p$ expressed in the body frame. Differentiating, and using Eqs. (2–4), gives a third kinematic equation for the mass particle:

$$\begin{aligned} \dot{\boldsymbol{r}}_p &= \dot{\mathcal{R}}^T \boldsymbol{R}_p + \mathcal{R}^T(\dot{\boldsymbol{X}}_p - \dot{\boldsymbol{X}}) \\ &= -\boldsymbol{\omega} \times \boldsymbol{r}_p + \boldsymbol{v}_p - \boldsymbol{v} \end{aligned} \tag{6}$$

Rearranging Eq. (6) gives the familiar expression for the velocity $\boldsymbol{v}_p$ of a point expressed in a rotating reference frame. The three representations $\boldsymbol{v}_p$, $\tilde{\boldsymbol{v}}_p$, and $\dot{\boldsymbol{r}}_p$ of the mass particle velocity correspond to three Hamiltonian models for the reduced system dynamics.

B. Dynamics

Buoyancy and gravity play important roles in underwater vehicle dynamics. A buoyant force $-mg\boldsymbol{I}_3$ acts on the body at its center of buoyancy (c.b.). For convenience, the c.b. is taken to be the origin of the body reference frame. A gravitational force $m_b g\boldsymbol{I}_3$ acts on the body at its c.g. The c.g. location is given, in the body frame, by the vector $\boldsymbol{r}_{\text{cg}}$. A gravitational force $m_p g\boldsymbol{I}_3$ acts on the particle of mass m_p. Here and throughout, it is assumed that the combined body/particle system is neutrally buoyant, that is,

$$m = m_b + m_p$$

This assumption preserves translational symmetry.

Let the body vector $\boldsymbol{u}$ denote the control force applied to the mass particle by the body, where $\boldsymbol{u}$ is chosen to preserve symmetries in the system dynamics. Let the inertial vector $\boldsymbol{H}_{\text{b/f}}$ represent the angular momentum of the body/fluid system about the origin of the inertial frame. Similarly, let the inertial vector $\boldsymbol{P}_{\text{b/f}}$ represent the linear momentum of the body/fluid system. Finally, let the inertial vector $\boldsymbol{P}_p$ represent the linear momentum of the mass particle. Assuming that no external forces or moments act, other than those caused by gravity and buoyancy, the dynamic equations in the inertial frame are

$$\dot{\boldsymbol{H}}_{\text{b/f}} = (\boldsymbol{X} + \mathcal{R}\boldsymbol{r}_{\text{cg}}) \times (m_b g\boldsymbol{I}_3) + \boldsymbol{X} \times (-mg\boldsymbol{I}_3) - \boldsymbol{X}_p \times \mathcal{R}\boldsymbol{u} \tag{7}$$

$$\dot{\boldsymbol{P}}_{\text{b/f}} = (m_b - m)g\boldsymbol{I}_3 - \mathcal{R}\boldsymbol{u} \tag{8}$$

$$\dot{\boldsymbol{P}}_p = m_p g\boldsymbol{I}_3 + \mathcal{R}\boldsymbol{u} \tag{9}$$

Notice in the equation for $\dot{\boldsymbol{P}}_{\text{b/f}}$ that the body experiences a vertically upward force of magnitude $m_p g$, whereas, in the equation for $\dot{\boldsymbol{P}}_p$ the mass particle experiences a vertically downward force of the same magnitude. When the two are coupled together through some physical actuator, for example, these two external forces will generally cancel. The moment caused by the separation between the c.b. and c.g. will remain, however.

Now let the inertial vector $\boldsymbol{H}_{\text{sys}}$ represent the angular momentum of the combined body/fluid/particle system about the origin of the inertial frame:

$$\boldsymbol{H}_{\text{sys}} = \boldsymbol{H}_{\text{b/f}} + \boldsymbol{X}_p \times \boldsymbol{P}_p$$

Similarly, let the inertial vector $\boldsymbol{P}_{\text{sys}}$ represent the linear momentum of the combined system:

$$\boldsymbol{P}_{\text{sys}} = \boldsymbol{P}_{\text{b/f}} + \boldsymbol{P}_p$$

In terms of these momenta, Eqs. (7–9) become

$$\dot{\boldsymbol{H}}_{\text{sys}} = (\boldsymbol{X} + \mathcal{R}\boldsymbol{r}_{\text{cg}}) \times (m_b g\boldsymbol{I}_3) + \boldsymbol{X} \times (-mg\boldsymbol{I}_3) + \boldsymbol{X}_p \times m_p g\boldsymbol{I}_3 \tag{10}$$

Table 1 Velocities, conjugate momenta, and inertia tensors

$\boldsymbol{\eta}$	$\boldsymbol{\nu}$	$\mathbb{I}_{\text{b/p}}$
$\begin{pmatrix} \boldsymbol{\omega} \\ \boldsymbol{v} \\ \boldsymbol{v}_p \end{pmatrix}$	$\begin{pmatrix} \boldsymbol{h}_{\text{b/f}} \\ \boldsymbol{p}_{\text{b/f}} \\ \boldsymbol{p}_p \end{pmatrix}$	$\begin{pmatrix} \boldsymbol{J}_b & m_b\hat{\boldsymbol{r}}_{\text{cg}} & \mathbb{0} \\ -m_b\hat{\boldsymbol{r}}_{\text{cg}} & m_b\mathbb{1} & \mathbb{0} \\ \mathbb{0} & \mathbb{0} & m_p\mathbb{1} \end{pmatrix}$
$\begin{pmatrix} \boldsymbol{\omega} \\ \boldsymbol{v} \\ \tilde{\boldsymbol{v}}_p \end{pmatrix}$	$\begin{pmatrix} \boldsymbol{h}_{\text{b/f}} \\ \boldsymbol{p}_{\text{sys}} \\ \boldsymbol{p}_p \end{pmatrix}$	$\begin{pmatrix} \boldsymbol{J}_b & m_b\hat{\boldsymbol{r}}_{\text{cg}} & \mathbb{0} \\ -m_b\hat{\boldsymbol{r}}_{\text{cg}} & m\mathbb{1} & m_p\mathbb{1} \\ \mathbb{0} & m_p\mathbb{1} & m_p\mathbb{1} \end{pmatrix}$
$\begin{pmatrix} \boldsymbol{\omega} \\ \boldsymbol{v} \\ \dot{\boldsymbol{r}}_p \end{pmatrix}$	$\begin{pmatrix} \boldsymbol{h}_{\text{sys}} \\ \boldsymbol{p}_{\text{sys}} \\ \boldsymbol{p}_p \end{pmatrix}$	$\begin{pmatrix} \boldsymbol{J}_b - m_p\hat{\boldsymbol{r}}_p\hat{\boldsymbol{r}}_p & m_b\hat{\boldsymbol{r}}_{\text{cg}} + m_p\hat{\boldsymbol{r}}_p & m_p\hat{\boldsymbol{r}}_p \\ -m_b\hat{\boldsymbol{r}}_{\text{cg}} - m_p\hat{\boldsymbol{r}}_p & (m_b + m_p)\mathbb{1} & m_p\mathbb{1} \\ -m_p\hat{\boldsymbol{r}}_p & m_p\mathbb{1} & m_p\mathbb{1} \end{pmatrix}$

$$\dot{\boldsymbol{P}}_{\text{sys}} = \boldsymbol{0} \tag{11}$$

$$\dot{\boldsymbol{P}}_p = m_p g\boldsymbol{I}_3 + \mathcal{R}\boldsymbol{u} \tag{12}$$

Notice on the right-hand side of Eq. (10) that the torque as a result of the internal force $\boldsymbol{u}$ has vanished, replaced by the torque as a result of the weight of the mass particle. Because the system is neutrally buoyant, all external forces vanish in Eq. (11).

To obtain reduced Hamiltonian models for the system dynamics, the equations are reexpressed in the body frame. To keep the presentation brief, it is convenient to define some unifying notation. Let $\boldsymbol{\eta}$ represent one of the generalized velocity vectors shown in the left-most column of Table 1. Let $\mathbb{I}_{\text{b/p}}$ represent the generalized inertia tensor in the corresponding row. Then the kinetic energy of the rigid-body/particle system is

$$T_{\text{b/p}} = \tfrac{1}{2}\boldsymbol{\eta}^T \mathbb{I}_{\text{b/p}}\boldsymbol{\eta} \tag{13}$$

Kirchhoff studied the irrotational motion of an unbounded volume of perfect fluid caused by the motion of an immersed rigid body.[16] He showed that the kinetic energy imparted to the fluid by the body's motion takes the form

$$T_f = \frac{1}{2}\begin{pmatrix} \boldsymbol{\omega} \\ \boldsymbol{v} \end{pmatrix}^T \begin{pmatrix} \boldsymbol{J}_f & \boldsymbol{C}_f \\ \boldsymbol{C}_f^T & \boldsymbol{M}_f \end{pmatrix} \begin{pmatrix} \boldsymbol{\omega} \\ \boldsymbol{v} \end{pmatrix}$$

where

$$\begin{pmatrix} \boldsymbol{J}_f & \boldsymbol{C}_f \\ \boldsymbol{C}_f^T & \boldsymbol{M}_f \end{pmatrix} = \begin{pmatrix} \boldsymbol{J}_f & \boldsymbol{C}_f \\ \boldsymbol{C}_f^T & \boldsymbol{M}_f \end{pmatrix}^T > 0$$

The component submatrices $\boldsymbol{J}_f$, $\boldsymbol{M}_f$, and $\boldsymbol{C}_f$ represent added inertia, added mass, and hydrodynamic coupling between the translational and rotational motion of the rigid body. These terms account for the energy necessary to accelerate the fluid around the body as it moves. Analytic expressions for these terms can be obtained, for simple shapes, as described in Ref. 17.

Define the generalized added inertia tensor

$$\mathbb{I}_f = \begin{pmatrix} \boldsymbol{J}_f & \boldsymbol{C}_f & \mathbb{0} \\ \boldsymbol{C}_f^T & \boldsymbol{M}_f & \mathbb{0} \\ \mathbb{0} & \mathbb{0} & \mathbb{0} \end{pmatrix} \tag{14}$$

so that

$$T_f = \tfrac{1}{2}\boldsymbol{\eta}^T \mathbb{I}_f\, \boldsymbol{\eta} \tag{15}$$

The total kinetic energy of the system is $T = T_{\text{b/p}} + T_f$.

With the total kinetic energy expressed with respect to the body frame, one can derive expressions for body momenta. The generalized momentum $\boldsymbol{\nu}$, which is conjugate to $\boldsymbol{\eta}$, is

$$\boldsymbol{\nu} = \frac{\partial T}{\partial \boldsymbol{\eta}} = (\mathbb{I}_{\text{b/p}} + \mathbb{I}_f)\boldsymbol{\eta} \tag{16}$$

Depending on the specific form of $\boldsymbol{\eta}$ and $\mathbb{I}_{\text{b/p}}$ chosen from Table 1, the components of $\boldsymbol{\nu}$ represent different momentum quantities.

In the following subsections, the various dynamic equations (7–12) are reexpressed in terms of body momenta. There are three sets of equations, each corresponding to a different parameterization ($\boldsymbol{v}_p$, $\tilde{\boldsymbol{v}}_p$, or $\dot{\boldsymbol{r}}_p$) of the mass particle velocity. In Sec. II.C, these three sets of equations will be recognized to have certain symmetries that allow the system dimension to be reduced.

1. Body-Frame Dynamic Equations Using $\boldsymbol{v}_p$

Referring to the generalized momentum vector $\boldsymbol{\nu}$ given in the first row of Table 1, the inertial and body-frame momenta are related as follows:

$$\boldsymbol{H}_{\mathrm{b/f}} = \mathcal{R}\boldsymbol{h}_{\mathrm{b/f}} + \boldsymbol{X} \times \boldsymbol{P}_{\mathrm{b/f}}, \qquad \boldsymbol{P}_{\mathrm{b/f}} = \mathcal{R}\boldsymbol{p}_{\mathrm{b/f}}, \qquad \boldsymbol{P}_p = \mathcal{R}\boldsymbol{p}_p \tag{17}$$

To obtain the equations of motion in the body frame, differentiate Eqs. (17) and substitute the kinematic expressions (2) and (3) where appropriate. Substituting on the left from Eqs. (7–9) and rearranging gives

$$\begin{aligned}
\dot{\boldsymbol{h}}_{\mathrm{b/f}} &= \boldsymbol{h}_{\mathrm{b/f}} \times \boldsymbol{\omega} + \boldsymbol{p}_{\mathrm{b/f}} \times \boldsymbol{v} + \boldsymbol{r}_{\mathrm{cg}} \times m_b g\left(\mathcal{R}^T \boldsymbol{I}_3\right) - \boldsymbol{r}_p \times \boldsymbol{u} \\
\dot{\boldsymbol{p}}_{\mathrm{b/f}} &= \boldsymbol{p}_{\mathrm{b/f}} \times \boldsymbol{\omega} + (m_b - m) g\left(\mathcal{R}^T \boldsymbol{I}_3\right) - \boldsymbol{u} \\
\dot{\boldsymbol{p}}_p &= \boldsymbol{p}_p \times \boldsymbol{\omega} + m_p g\left(\mathcal{R}^T \boldsymbol{I}_3\right) + \boldsymbol{u}
\end{aligned} \tag{18}$$

2. Body-Frame Dynamic Equations Using $\tilde{\boldsymbol{v}}_p$

Referring to the generalized momentum vector $\boldsymbol{\nu}$ given in the second row of Table 1, one finds

$$\begin{aligned}
\boldsymbol{H}_{\mathrm{b/f}} &= \mathcal{R}\boldsymbol{h}_{\mathrm{b/f}} + \boldsymbol{X} \times (\boldsymbol{P}_{\mathrm{sys}} - \boldsymbol{P}_p) \\
\boldsymbol{P}_{\mathrm{sys}} &= \mathcal{R}\boldsymbol{p}_{\mathrm{sys}}, \qquad \boldsymbol{P}_p = \mathcal{R}\boldsymbol{p}_p
\end{aligned} \tag{19}$$

Differentiating Eqs. (19) and using the kinematic equations (2) and (3) and the inertial dynamics (7), (11), and (12) give a second set of dynamic equations in the body frame:

$$\begin{aligned}
\dot{\boldsymbol{h}}_{\mathrm{b/f}} &= \boldsymbol{h}_{\mathrm{b/f}} \times \boldsymbol{\omega} + \boldsymbol{p}_{\mathrm{sys}} \times \boldsymbol{v} - \boldsymbol{p}_p \times \boldsymbol{v} + \boldsymbol{r}_{\mathrm{cg}} \times m_b g\left(\mathcal{R}^T \boldsymbol{I}_3\right) - \boldsymbol{r}_p \times \boldsymbol{u} \\
\dot{\boldsymbol{p}}_{\mathrm{sys}} &= \boldsymbol{p}_{\mathrm{sys}} \times \boldsymbol{\omega}, \qquad \dot{\boldsymbol{p}}_p = \boldsymbol{p}_p \times \boldsymbol{\omega} + m_p g\left(\mathcal{R}^T \boldsymbol{I}_3\right) + \boldsymbol{u}
\end{aligned} \tag{20}$$

3. Body-Frame Dynamic Equations Using $\dot{\boldsymbol{r}}_p$

Referring to the generalized momentum vector $\boldsymbol{\nu}$ given in the third row of Table 1,

$$\boldsymbol{H}_{\mathrm{sys}} = \mathcal{R}\boldsymbol{h}_{\mathrm{sys}} + \boldsymbol{X} \times \boldsymbol{P}_{\mathrm{sys}}, \qquad \boldsymbol{P}_{\mathrm{sys}} = \mathcal{R}\boldsymbol{p}_{\mathrm{sys}}, \qquad \boldsymbol{P}_p = \mathcal{R}\boldsymbol{p}_p \tag{21}$$

Differentiating Eqs. (21) and using the kinematic equations (2) and (3) and the inertial dynamics (10–12) give a third set of dynamic equations in the body frame:

$$\begin{aligned}
\dot{\boldsymbol{h}}_{\mathrm{sys}} &= \boldsymbol{h}_{\mathrm{sys}} \times \boldsymbol{\omega} + \boldsymbol{p}_{\mathrm{sys}} \times \boldsymbol{v} + \boldsymbol{r}_{\mathrm{cg}} \times m_b g\left(\boldsymbol{R}^T \boldsymbol{I}_3\right) + \boldsymbol{r}_p \times m_p g\left(\boldsymbol{R}^T \boldsymbol{I}_3\right) \\
\dot{\boldsymbol{p}}_{\mathrm{sys}} &= \boldsymbol{p}_{\mathrm{sys}} \times \boldsymbol{\omega}, \qquad \dot{\boldsymbol{p}}_p = \boldsymbol{p}_p \times \boldsymbol{\omega} + m_p g\left(\boldsymbol{R}^T \boldsymbol{I}_3\right) + \boldsymbol{u}
\end{aligned} \tag{22}$$

C. Reduced Hamiltonian Models

Three sets of body-frame dynamic equations were described in Sec. II.B, corresponding to three representations ($\boldsymbol{v}_p$, $\tilde{\boldsymbol{v}}_p$, and $\dot{\boldsymbol{r}}_p$) of the point-mass velocity. Each set of equations exhibits symmetry under arbitrary translations of the inertial frame and arbitrary rotations of the inertial frame about the direction of gravity. As a consequence, it is not necessary to retain the complete set of kinematic equations in order to express the dynamics. Because of translational symmetry, for example, the inertial position of the body plays no role in the dynamic equations; as far as the dynamics are concerned, one can disregard the translational kinematic equation (3). The inertial position of the mass particle is also irrelevant; however, its position relative to the body certainly matters. Because of rotational symmetry about the inertial vertical direction, the dynamic equations do not require full attitude information. Define the body vector

$$\boldsymbol{\gamma} = \mathcal{R}^T \boldsymbol{I}_3 \tag{23}$$

which is simply the direction of gravity expressed in the body frame. Because the external forces and torques appearing in the dynamic equations depend only on $\boldsymbol{\gamma}$, one can replace the matrix differential equation (2) with the simpler rotational kinematic equation

$$\dot{\boldsymbol{\gamma}} = \boldsymbol{\gamma} \times \boldsymbol{\omega}$$

Define the Hamiltonian

$$\mathcal{H}(z) = \tfrac{1}{2}\boldsymbol{\nu}^T \left(\mathbb{I}_{\mathrm{b/p}} + \mathbb{I}_f\right)^{-1} \boldsymbol{\nu} - (m_b g \boldsymbol{r}_{\mathrm{cg}} + m_p g \boldsymbol{r}_p) \cdot \gamma \tag{24}$$

where three possible choices of $\boldsymbol{\nu}$ and $\mathbb{I}_{\mathrm{b/p}}$ are given in Table 1 and where $\boldsymbol{z}$ is given in the corresponding row of Table 2.

Proposition 2.1: The coupled motion of a rigid body and a mass particle in an ideal fluid is described by the noncanonical Hamiltonian control system (1). Three such models correspond to the three choices of generalized velocity $\boldsymbol{\eta}$ and generalized inertia tensor $\mathbb{I}_{\mathrm{b/p}}$ given in Table 1. For each model, the Hamiltonian $\mathcal{H}$ is given by Eq. (24). The state vector $\boldsymbol{z}$, the Poisson tensor $\boldsymbol{\Lambda}$, and the input matrix $\boldsymbol{G}$ are given in the row of Table 2, which corresponds to the choice of $\boldsymbol{\eta}$ and $\mathbb{I}_{\mathrm{b/p}}$ in Table 1. Three independent Casimirs for each of these three models are given in Table 2.

Table 2 Poisson tensors, input matrices, and Casimirs

z	$\boldsymbol{\Lambda}$	$\boldsymbol{G}$	C_1	C_2	C_3
$\begin{pmatrix} \boldsymbol{h}_{\mathrm{b/f}} \\ \boldsymbol{p}_{\mathrm{b/f}} \\ \boldsymbol{\gamma} \\ \boldsymbol{r}_p \\ \boldsymbol{p}_p \end{pmatrix}$	$\begin{pmatrix} \hat{\boldsymbol{h}}_{\mathrm{b/f}} & \hat{\boldsymbol{p}}_{\mathrm{b/f}} & \hat{\boldsymbol{\gamma}} & \hat{\boldsymbol{r}}_p & \hat{\boldsymbol{p}}_p \\ \hat{\boldsymbol{p}}_{\mathrm{b/f}} & 0 & 0 & \mathbb{1} & 0 \\ \hat{\boldsymbol{\gamma}} & 0 & 0 & 0 & 0 \\ \hat{\boldsymbol{r}}_p & -\mathbb{1} & 0 & 0 & \mathbb{1} \\ \hat{\boldsymbol{p}}_p & 0 & 0 & -\mathbb{1} & 0 \end{pmatrix}$	$\begin{pmatrix} -\hat{\boldsymbol{r}}_p \\ -\mathbb{1} \\ 0 \\ 0 \\ \mathbb{1} \end{pmatrix}$	$(\boldsymbol{p}_{\mathrm{b/f}} + \boldsymbol{p}_p) \cdot (\boldsymbol{p}_{\mathrm{b/f}} + \boldsymbol{p}_p)$	$\boldsymbol{\gamma} \cdot (\boldsymbol{p}_{\mathrm{b/f}} + \boldsymbol{p}_p)$	$\boldsymbol{\gamma} \cdot \boldsymbol{\gamma}$
$\begin{pmatrix} \boldsymbol{h}_{\mathrm{b/f}} \\ \boldsymbol{p}_{\mathrm{sys}} \\ \boldsymbol{\gamma} \\ \boldsymbol{r}_p \\ \boldsymbol{p}_p \end{pmatrix}$	$\begin{pmatrix} \hat{\boldsymbol{h}}_{\mathrm{b/f}} & \hat{\boldsymbol{p}}_{\mathrm{sys}} & \hat{\boldsymbol{\gamma}} & \hat{\boldsymbol{r}}_p & \hat{\boldsymbol{p}}_p \\ \hat{\boldsymbol{p}}_{\mathrm{sys}} & 0 & 0 & 0 & 0 \\ \hat{\boldsymbol{\gamma}} & 0 & 0 & 0 & 0 \\ \hat{\boldsymbol{r}}_p & 0 & 0 & 0 & \mathbb{1} \\ \hat{\boldsymbol{p}}_p & 0 & 0 & -\mathbb{1} & 0 \end{pmatrix}$	$\begin{pmatrix} -\hat{\boldsymbol{r}}_p \\ 0 \\ 0 \\ 0 \\ \mathbb{1} \end{pmatrix}$	$\boldsymbol{p}_{\mathrm{sys}} \cdot \boldsymbol{p}_{\mathrm{sys}}$	$\boldsymbol{\gamma} \cdot \boldsymbol{p}_{\mathrm{sys}}$	$\boldsymbol{\gamma} \cdot \boldsymbol{\gamma}$
$\begin{pmatrix} \boldsymbol{h}_{\mathrm{sys}} \\ \boldsymbol{p}_{\mathrm{sys}} \\ \boldsymbol{\gamma} \\ \boldsymbol{r}_p \\ \boldsymbol{p}_p \end{pmatrix}$	$\begin{pmatrix} \hat{\boldsymbol{h}}_{\mathrm{sys}} & \hat{\boldsymbol{p}}_{\mathrm{sys}} & \hat{\boldsymbol{\gamma}} & 0 & 0 \\ \hat{\boldsymbol{p}}_{\mathrm{sys}} & 0 & 0 & 0 & 0 \\ \hat{\boldsymbol{\gamma}} & 0 & 0 & 0 & 0 \\ 0 & 0 & 0 & 0 & \mathbb{1} \\ 0 & 0 & 0 & -\mathbb{1} & 0 \end{pmatrix}$	$\begin{pmatrix} 0 \\ 0 \\ 0 \\ 0 \\ \mathbb{1} \end{pmatrix}$	$\boldsymbol{p}_{\mathrm{sys}} \cdot \boldsymbol{p}_{\mathrm{sys}}$	$\boldsymbol{\gamma} \cdot \boldsymbol{p}_{\mathrm{sys}}$	$\boldsymbol{\gamma} \cdot \boldsymbol{\gamma}$

Straightforward computations verify that the Hamiltonian models given in Proposition 2.1 correspond to the dynamic equations given in Sec. II.B. The proof is omitted.

Remark 2.2: As explained in Sec. I, a Casimir function is one whose gradient lies in the null space of $\boldsymbol{\Lambda}$. Because there are three independent Casimirs for the system in Proposition 2.1, the 15×15 Poisson tensor $\boldsymbol{\Lambda}$ has at most rank 12. In fact, $\boldsymbol{\Lambda}$ has exactly rank 12 for generic values of z. Whereas the Hamiltonian is conserved when $\boldsymbol{u} = \boldsymbol{0}$, the Casimirs are conserved even when $\boldsymbol{u} \neq \boldsymbol{0}$. They correspond to inertial momentum conservation laws, which are unaffected by internal forces. The rank deficiency of $\boldsymbol{\Lambda}$ reflects these inertial conservation laws in the reduced-dimensional dynamics.

Remark 2.3: One can include a conservative internal force $\boldsymbol{u} = -\nabla U(\boldsymbol{r}_p)$ in the Hamiltonian formulation of Proposition 2.1. Such a force couples the mass particle dynamics to those of the body. The potential function $U(\boldsymbol{r}_p)$ is simply appended to the Hamiltonian (24).

Remark 2.4: The Hamiltonian model defined by the last row in Tables 1 and 2 is related to the unconstrained, reduced Lagrangian system described in Ref. 18. The Lagrange–Poincaré equations given there were derived through a formal reduction process in which the dynamics are recognized to be invariant under the action of a Lie group. See Ref. 12 or 19 for a discussion of Lagrangian and Hamiltonian reduction and the special role of Lie groups.

Remark 2.5: In the absence of gravity, weight and buoyancy vanish, and the system exhibits symmetry under arbitrary translations and rotations of the inertial reference frame. In this case, $\boldsymbol{\gamma}$ is superfluous, and the dimension of the system reduces further. The dynamics are still Hamiltonian in the sense of Eq. (1); however, the dimensions of $\boldsymbol{\Lambda}$ and $\boldsymbol{G}$ drop by three, and the Hamiltonian becomes simply the kinetic energy:

$$H = \tfrac{1}{2}\boldsymbol{\nu}^T\left(\mathbb{I}_{\mathrm{b/p}} + \mathbb{I}_f\right)^{-1}\boldsymbol{\nu}$$

The special case of a rigid spacecraft with a moving point mass is obtained by setting $\mathbb{I}_f$ equal to zero. Because $\boldsymbol{\gamma}$ is no longer a state component, the Casimirs C_2 and C_3 vanish. The square magnitude of linear momentum C_1 remains a Casimir, and a new Casimir is generated:

$$\begin{aligned} C_4 &= (\boldsymbol{h}_{\mathrm{b/f}} + \boldsymbol{r}_p \times \boldsymbol{p}_p)\cdot(\boldsymbol{p}_{\mathrm{b/f}} + \boldsymbol{p}_p) \\ &= (\boldsymbol{h}_{\mathrm{b/f}} + \boldsymbol{r}_p \times \boldsymbol{p}_p)\cdot \boldsymbol{p}_{\mathrm{sys}} \\ &= \boldsymbol{h}_{\mathrm{sys}} \cdot \boldsymbol{p}_{\mathrm{sys}} \end{aligned}$$

D. Example Application

As an example, consider the problem of stabilizing steady long-axis descent of a prolate spheroid using a moving point mass and potential-shaping feedback. The example, which first appeared in Ref. 20, is intended as a simple illustration of moving mass control and the utility of Hamiltonian models for this purpose. More meaningful and sophisticated applications are being investigated.

For a prolate spheroid with the body frame fixed in the ellipsoid principal axes, the added inertia matrix $\boldsymbol{J}_f$ and the added mass matrix $\boldsymbol{M}_f$ are diagonal, and the hydrodynamic coupling matrix $\boldsymbol{C}_f$ vanishes. If one assumes that the mass of the body is uniformly distributed, then $\boldsymbol{r}_{\mathrm{cg}} = \boldsymbol{0}$, and the inertia matrix $\boldsymbol{J}_b$ is diagonal. Assume that the axis of axial symmetry is the $\boldsymbol{b}_3$ axis. Then $\boldsymbol{M}_f = \mathrm{diag}(m_1, m_1, m_3)$, where $m_1 > m_3 > 0$.

Define the potential-shaping control law

$$\boldsymbol{u}_{\mathrm{int}} = -\boldsymbol{K}\boldsymbol{r}_p$$

where $\boldsymbol{K} = \mathrm{diag}(k_1, k_2, k_3)$ is a control gain matrix parameterizing the artificial potential function

$$U(\boldsymbol{r}_p) = \tfrac{1}{2}\boldsymbol{r}_p^T\boldsymbol{K}\boldsymbol{r}_p$$

If $\boldsymbol{K}$ were a multiple of the identity, then $\boldsymbol{u}_{\mathrm{int}}$ would be a central force. In this case, the "actuator" might be a simple spherical pendulum with a linear spring. As stated in Proposition 2.1 and Remark 2.3, the closed-loop system is Hamiltonian with

$$\mathcal{H}_U(z) = \tfrac{1}{2}\boldsymbol{\nu}^T(\mathbb{I}_{\mathrm{b/p}} + \mathbb{I}_f)^{-1}\boldsymbol{\nu} - m_p g \boldsymbol{r}_p \cdot \boldsymbol{\gamma} + \tfrac{1}{2}\boldsymbol{r}_p^T\boldsymbol{K}\boldsymbol{r}_p$$

The Hamiltonian dynamics are

$$\dot{z} = \boldsymbol{\Lambda}(z)\nabla\mathcal{H}_U(z)$$

where z and $\boldsymbol{\Lambda}$ are chosen, for example, from the first row of Table 2. Consider the equilibrium

$$\boldsymbol{h}_{\mathrm{b/f}}|_{\mathrm{eq}} = \boldsymbol{0}, \qquad \boldsymbol{p}_{\mathrm{b/f}}|_{\mathrm{eq}} = (m_b + m_3)v_3^0\boldsymbol{e}_3$$

$$\boldsymbol{\gamma}|_{\mathrm{eq}} = \boldsymbol{e}_3, \qquad \boldsymbol{r}_p|_{\mathrm{eq}} = (m_p g/k_3)\boldsymbol{e}_3, \qquad \boldsymbol{p}_p|_{\mathrm{eq}} = m_p v_3^0\boldsymbol{e}_3 \quad (25)$$

where $k_3 > 0$. This equilibrium corresponds to steady descent at speed v_3^0 with the $\boldsymbol{b}_3$ axis vertical and with the point mass m_p "hanging" a distance $m_p g/k_3$ below the c.b.

One may find conditions for nonlinear stability using the energy-Casimir method.[12] This involves constructing a function $H_\Phi = H_U + \Phi(C_1, C_2, C_3)$, which has a strict minimum or maximum at the equilibrium. The function H_Φ is conserved by construction, so that it is automatically a Lyapunov function.

Proposition 2.6: The equilibrium (25) is stable if

$$k_3 < \bar{k}_3 = \frac{(m_p g)^2}{(m_1 - m_3)\left(v_3^0\right)^2}, \qquad k_i > \frac{\bar{k}_3 k_3}{\bar{k}_3 - k_3}, \qquad \text{for} \qquad i = 1, 2$$

Proof: A Lyapunov function for the equilibrium (25), obtained using the energy-Casimir method, is

$$\begin{aligned} \mathcal{H}_\Phi(z) = \mathcal{H}_U(z) - v_3^0 C_2 + \tfrac{1}{2}(m + m_3)\left(v_3^0\right)^2(1 + \bar{k}_3/k_3)C_3 \\ - \tfrac{1}{2}\left[(m_p g)^2\big/k_3\right](C_3 - 1)^2 \end{aligned}$$

The terms C_2 and C_3 are the Casimirs given in the first row of Table 2. Nonlinear stability of the equilibrium follows from Lyapunov's direct method. □

The energy-Casimir method only provides a sufficient condition for stability. Failure to construct a Lyapunov function does not imply that the equilibrium is unstable. The process of constructing such a function can be more or less difficult depending on the choice of $\boldsymbol{\nu}$ and $\mathbb{I}_{\mathrm{b/p}}$. For this example, choosing $\boldsymbol{\nu}$ and $\mathbb{I}_{\mathrm{b/p}}$ from the first row of Table 1 made the analysis straightforward. This choice corresponds to a decoupled view of the body/fluid and particle kinetic energies.

The result in Proposition 2.6 is reminiscent of stability results in Ref. 21, where it was shown that long-axis descent of a bottom-heavy prolate spheroid is stable provided the (fixed) c.g. is sufficiently low. In the present context, this requirement corresponds to making the "spring stiffness" k_3 sufficiently small. Intuitively, the remaining gains k_1 and k_2 should be large enough to prevent large lateral oscillations of the point mass.

III. Mass Particle Constrained to a Linear Track

This section considers the case of a mass particle, which is constrained to move along a linear track fixed with respect to the body. Without loss of generality, assume that this track is parallel to the $\boldsymbol{b}_1$ axis (see Fig. 2). In the interest of brevity, derivations of the equations of motion are omitted. For the special case of a spacecraft, the equations are derived in Ref. 22. Section II provides sufficient guidance to generalize this derivation to the case of an underwater vehicle.

A. Reduced Hamiltonian Models

In this section, we redefine $\boldsymbol{\eta}$ so that its final component is the scalar component of mass particle velocity along the track. Thus $\boldsymbol{\eta}$ becomes 7×1 rather than 9×1 (see Table 3). Once again, $\mathbb{I}_{\mathrm{b/p}}$ represents the generalized inertia tensor, now 7×7. We also redefine $\mathbb{I}_f$ by removing the last two rows and columns of zeros in Eq. (14). The kinetic energy of the system is

$$T = \tfrac{1}{2}\boldsymbol{\eta}^T(\mathbb{I}_{\mathrm{b/p}} + \mathbb{I}_f)\boldsymbol{\eta}$$

Table 3 Velocities, conjugate momenta, and inertia tensors

$\boldsymbol{\eta}$	$\boldsymbol{\nu}$	$\mathbb{I}_{\mathrm{b/p}}$
$\begin{pmatrix}\boldsymbol{\omega}\\ \boldsymbol{v}\\ v_{p_1}\end{pmatrix}$	$\begin{pmatrix}\bar{\boldsymbol{h}}\\ \bar{\boldsymbol{p}}\\ p_{p_1}\end{pmatrix}$	$\begin{pmatrix}\boldsymbol{J}_b - m_p\hat{\boldsymbol{r}}_p\mathbb{1}_{23}\hat{\boldsymbol{r}}_p & m_b\hat{\boldsymbol{r}}_{\mathrm{cg}} + m_p\hat{\boldsymbol{r}}_p\mathbb{1}_{23} & \mathbf{0}\\ -m_b\hat{\boldsymbol{r}}_{\mathrm{cg}} - m_p\mathbb{1}_{23}\hat{\boldsymbol{r}}_p & m_b\mathbb{1} + m_p\mathbb{1}_{23} & \mathbf{0}\\ \mathbf{0}^T & \mathbf{0}^T & m_p\end{pmatrix}$
$\begin{pmatrix}\boldsymbol{\omega}\\ \boldsymbol{v}\\ \tilde{v}_{p_1}\end{pmatrix}$	$\begin{pmatrix}\bar{\boldsymbol{h}}\\ \boldsymbol{p}_{\mathrm{sys}}\\ p_{p_1}\end{pmatrix}$	$\begin{pmatrix}\boldsymbol{J}_b - m_p\hat{\boldsymbol{r}}_p\mathbb{1}_{23}\hat{\boldsymbol{r}}_p & m_b\hat{\boldsymbol{r}}_{\mathrm{cg}} + m_p\hat{\boldsymbol{r}}_p\mathbb{1}_{23} & \mathbf{0}\\ -m_b\hat{\boldsymbol{r}}_{\mathrm{cg}} - m_p\mathbb{1}_{23}\hat{\boldsymbol{r}}_p & m\mathbb{1} & m_p\boldsymbol{e}_1\\ \mathbf{0}^T & m_p\boldsymbol{e}_1^T & m_p\end{pmatrix}$
$\begin{pmatrix}\boldsymbol{\omega}\\ \boldsymbol{v}\\ \dot{r}_{p_1}\end{pmatrix}$	$\begin{pmatrix}\boldsymbol{h}_{\mathrm{sys}}\\ \boldsymbol{p}_{\mathrm{sys}}\\ p_{p_1}\end{pmatrix}$	$\begin{pmatrix}\boldsymbol{J}_b - m_p\hat{\boldsymbol{r}}_p\hat{\boldsymbol{r}}_p & m_b\hat{\boldsymbol{r}}_{\mathrm{cg}} + m_p\hat{\boldsymbol{r}}_p & m_p\hat{\boldsymbol{r}}_p\boldsymbol{e}_1\\ -m_b\hat{\boldsymbol{r}}_{\mathrm{cg}} - m_p\hat{\boldsymbol{r}}_p & m\mathbb{1} & m_p\boldsymbol{e}_1\\ -m_p\boldsymbol{e}_1^T\hat{\boldsymbol{r}}_p & m_p\boldsymbol{e}_1^T & m_p\end{pmatrix}$

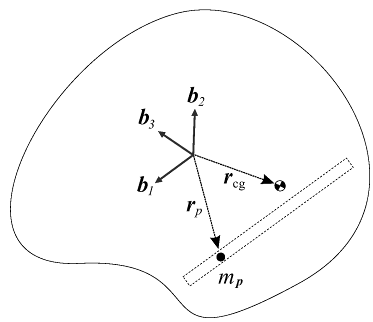

Fig. 2 Rigid body and a moving mass-particle constrained to a linear track.

The generalized momentum $\boldsymbol{\nu}$, which is conjugate to $\boldsymbol{\eta}$, is given, once again, by Eq. (16). The overbar in some of the components of $\boldsymbol{\nu}$ denotes that the given momentum term includes contributions from the body's motion, the fluid's motion, and the mass particle's motion in directions orthogonal to the track.

Proceeding as in Sec. II.B, one can express the dynamics in the body frame using any one of the three generalized momentum vectors $\boldsymbol{\nu}$ given in Table 3. Each set of dynamic equations exhibits symmetry under arbitrary translations of the inertial frame and arbitrary rotations of the inertial frame about the direction of gravity. In each case, the dynamics can be expressed as a noncanonical Hamiltonian control system in the form (1).

Define the Hamiltonian

$$\mathcal{H}(z) = \tfrac{1}{2}\boldsymbol{\nu}^T(\mathbb{I}_{\mathrm{b/p}} + \mathbb{I}_f)^{-1}\boldsymbol{\nu} - (m_b g\boldsymbol{r}_{\mathrm{cg}} + m_p g\boldsymbol{r}_p)\cdot\boldsymbol{\gamma} \tag{26}$$

where it is understood that only the first element of $\boldsymbol{r}_p$ can vary with time.

Proposition 3.1: The coupled motion of a rigid body in a fluid and a mass particle constrained along a linear track, as just outlined, is described by the noncanonical Hamiltonian control system (1). Three such models correspond to the three choices of generalized velocity $\boldsymbol{\eta}$ and generalized inertia tensor $\mathbb{I}_{\mathrm{b/p}}$ given in Table 3. For each model, the Hamiltonian $\mathcal{H}$ is given by Eq. (26). The state vector z, the Poisson tensor $\boldsymbol{\Lambda}$, and the input matrix $\boldsymbol{G}$ are given in the row of Table 4, which corresponds to the choice of $\boldsymbol{\eta}$ and $\mathbb{I}_{\mathrm{b/p}}$ in Table 3. Three independent Casimirs for each of these models are given in Table 5.

Remark 3.2: Because there are three independent Casimirs for the system in Proposition 3.1, the 11×11 Poisson tensor $\boldsymbol{\Lambda}$ has at most rank eight. In fact, $\boldsymbol{\Lambda}$ has exactly rank eight for generic values of z (see Remark 2.2).

Remark 2.5 applies here, as well. In the absence of gravity, the system dimension reduces further. Letting $\mathbb{I}_f$ be zero gives the equations for a rigid spacecraft with a mass particle confined to move along a track.

B. Example Application

The following example, which also appeared in Ref. 23, considers nonlinear stability of steady major axis rotation of a rigid body with a spring-mass oscillator. Because of its practical implications for spacecraft with precession or nutation dampers, this problem is well studied (see Ref. 24 and references therein). Despite considerable attention, however, there appears to be no proof, prior to this example, of nonlinear stability.

Figure 3 depicts a rigid body and two point masses. A reference frame is fixed at the c.g. of the rigid body. The reference frame is chosen to coincide with the principal axes of inertia so that the rigid-body inertia tensor $\tilde{\boldsymbol{J}}_b$ is diagonal. A point mass m_p is fixed at the point $\boldsymbol{r}_0 = [0, 0, -\Delta]^T$, with respect to the body reference frame. Another point mass m_p is located at $\boldsymbol{r}_p = [r_{p_1}, 0, \Delta]^T$; this point mass moves, under the influence of a force u, along a track parallel to the $\boldsymbol{b}_1$ axis. The mass of the complete system is m. We assume that this system operates in a vacuum ($\mathbb{I}_f$ is zero) and away from the effects of gravity.

Table 4 Poisson tensors and input matrices

z	$\boldsymbol{\Lambda}$	$\boldsymbol{G}$
$\begin{pmatrix}\bar{\boldsymbol{h}}\\ \bar{\boldsymbol{p}}\\ \boldsymbol{\gamma}\\ r_{p_1}\\ p_{p_1}\end{pmatrix}$	$\begin{pmatrix}\hat{\bar{\boldsymbol{h}}} + \widehat{\left(\hat{\boldsymbol{r}}_p p_{p_1}\boldsymbol{e}_1\right)} & \hat{\bar{\boldsymbol{p}}} + p_{p_1}\hat{\boldsymbol{e}}_1 & \hat{\boldsymbol{\gamma}} & \hat{\boldsymbol{r}}_p\boldsymbol{e}_1 & \mathbf{0}\\ \hat{\bar{\boldsymbol{p}}} + p_{p_1}\hat{\boldsymbol{e}}_1 & \mathbb{0} & \mathbb{0} & \boldsymbol{e}_1 & \mathbf{0}\\ \hat{\boldsymbol{\gamma}} & \mathbb{0} & \mathbb{0} & \mathbf{0} & \mathbf{0}\\ -\boldsymbol{e}_1^T\hat{\boldsymbol{r}}_p & -\boldsymbol{e}_1^T & \mathbf{0}^T & 0 & 1\\ \mathbf{0}^T & \mathbf{0}^T & \mathbf{0}^T & -1 & 0\end{pmatrix}$	$\begin{pmatrix}-\hat{\boldsymbol{r}}_p\boldsymbol{e}_1\\ -\boldsymbol{e}_1\\ \mathbf{0}\\ 0\\ 1\end{pmatrix}$
$\begin{pmatrix}\bar{\boldsymbol{h}}\\ \boldsymbol{p}_{\mathrm{sys}}\\ \boldsymbol{\gamma}\\ r_{p_1}\\ p_{p_1}\end{pmatrix}$	$\begin{pmatrix}\hat{\bar{\boldsymbol{h}}} + \widehat{\left(\hat{\boldsymbol{r}}_p p_{p_1}\boldsymbol{e}_1\right)} & \hat{\boldsymbol{p}}_{\mathrm{sys}} & \hat{\boldsymbol{\gamma}} & \hat{\boldsymbol{r}}_p\boldsymbol{e}_1 & \mathbf{0}\\ \hat{\boldsymbol{p}}_{\mathrm{sys}} & \mathbb{0} & \mathbb{0} & \mathbf{0} & \mathbf{0}\\ \hat{\boldsymbol{\gamma}} & \mathbb{0} & \mathbb{0} & \mathbf{0} & \mathbf{0}\\ -\boldsymbol{e}_1^T\hat{\boldsymbol{r}}_p & \mathbf{0}^T & \mathbf{0}^T & 0 & 1\\ \mathbf{0}^T & \mathbf{0}^T & \mathbf{0}^T & -1 & 0\end{pmatrix}$	$\begin{pmatrix}-\hat{\boldsymbol{r}}_p\boldsymbol{e}_1\\ \mathbf{0}\\ \mathbf{0}\\ 0\\ 1\end{pmatrix}$
$\begin{pmatrix}\boldsymbol{h}_{\mathrm{sys}}\\ \boldsymbol{p}_{\mathrm{sys}}\\ \boldsymbol{\gamma}\\ r_{p_1}\\ p_{p_1}\end{pmatrix}$	$\begin{pmatrix}\hat{\boldsymbol{h}}_{\mathrm{sys}} & \hat{\boldsymbol{p}}_{\mathrm{sys}} & \hat{\boldsymbol{\gamma}} & \mathbf{0} & \mathbf{0}\\ \hat{\boldsymbol{p}}_{\mathrm{sys}} & \mathbb{0} & \mathbb{0} & \mathbf{0} & \mathbf{0}\\ \hat{\boldsymbol{\gamma}} & \mathbb{0} & \mathbb{0} & \mathbf{0} & \mathbf{0}\\ \mathbf{0}^T & \mathbf{0}^T & \mathbf{0}^T & 0 & 1\\ \mathbf{0}^T & \mathbf{0}^T & \mathbf{0}^T & -1 & 0\end{pmatrix}$	$\begin{pmatrix}\mathbf{0}\\ \mathbf{0}\\ \mathbf{0}\\ 0\\ 1\end{pmatrix}$

Table 5 Casimir functions

$\boldsymbol{\nu}$	C_1	C_2	C_3
$\begin{pmatrix}\bar{\boldsymbol{h}}\\ \bar{\boldsymbol{p}}\\ p_{p_1}\end{pmatrix}$	$(\bar{\boldsymbol{p}} + p_{p_1}\boldsymbol{e}_1)\cdot(\bar{\boldsymbol{p}} + p_{p_1}\boldsymbol{e}_1)$	$\boldsymbol{\gamma}\cdot(\bar{\boldsymbol{p}} + p_{p_1}\boldsymbol{e}_1)$	$\boldsymbol{\gamma}\cdot\boldsymbol{\gamma}$
$\begin{pmatrix}\bar{\boldsymbol{h}}\\ \boldsymbol{p}_{\mathrm{sys}}\\ p_{p_1}\end{pmatrix}$	$\boldsymbol{p}_{\mathrm{sys}}\cdot\boldsymbol{p}_{\mathrm{sys}}$	$\boldsymbol{\gamma}\cdot\boldsymbol{p}_{\mathrm{sys}}$	$\boldsymbol{\gamma}\cdot\boldsymbol{\gamma}$
$\begin{pmatrix}\boldsymbol{h}_{\mathrm{sys}}\\ \boldsymbol{p}_{\mathrm{sys}}\\ p_{p_1}\end{pmatrix}$	$\boldsymbol{p}_{\mathrm{sys}}\cdot\boldsymbol{p}_{\mathrm{sys}}$	$\boldsymbol{\gamma}\cdot\boldsymbol{p}_{\mathrm{sys}}$	$\boldsymbol{\gamma}\cdot\boldsymbol{\gamma}$

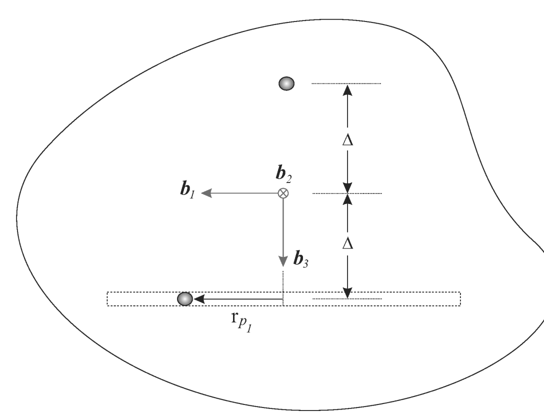

Fig. 3 Rigid body and a moving point mass.

Referring to the generalized inertia tensor $\mathbb{I}_{\mathrm{b/p}}$ in the third row of Table 3, the combined inertia of the rigid body, the fixed point mass, and the moving point mass is

$$\begin{aligned} \boldsymbol{J}_b - m_p\hat{\boldsymbol{r}}_p^2 &= \tilde{\boldsymbol{J}}_b - m_p\hat{\boldsymbol{r}}_0^2 - m_p\hat{\boldsymbol{r}}_p^2 \\ &= \begin{pmatrix} J_1 & 0 & -m_p\Delta r_{p_1} \\ 0 & J_2 + m_p r_{p_1}^2 & 0 \\ -m_p\Delta r_{p_1} & 0 & J_3 + m_p r_{p_1}^2 \end{pmatrix} \end{aligned}$$

where

$$J_1 = \tilde{J}_1 + 2m_p\Delta^2, \qquad J_2 = \tilde{J}_2 + 2m_p\Delta^2, \qquad J_3 = \tilde{J}_3$$

We will assume that $J_1 > J_2$ and $J_1 > J_3$.

The system kinetic energy is $\frac{1}{2}\boldsymbol{\eta}^T\mathbb{I}_{\mathrm{b/p}}\boldsymbol{\eta}$, where $\boldsymbol{\eta}$ is also given in the third row of Table 3. Suppose, as in Remark 2.3, that we define

$$U(r_{p_1}) = \tfrac{1}{2}kr_{p_1}^2$$

and let

$$u = -\frac{\mathrm{d}U}{\mathrm{d}r_{p_1}} = -kr_{p_1} \tag{27}$$

This internal force can correspond to the linear spring force in a precession damper, for example, where $k > 0$ is the spring's stiffness. The closed-loop dynamics are Hamiltonian with respect to

$$\mathcal{H}_U(z) = \mathcal{H}(z) + U(r_{p_1})$$

We consider stability of the equilibrium motion

$$\boldsymbol{h}_{\mathrm{sys}}|_{\mathrm{eq}} = h_1^0\boldsymbol{e}_1, \qquad \boldsymbol{p}_{\mathrm{sys}}|_{\mathrm{eq}} = \boldsymbol{0}, \qquad r_{p_1}|_{\mathrm{eq}} = 0, \qquad p_{p_1}|_{\mathrm{eq}} = 0 \tag{28}$$

This equilibrium corresponds to steady rotation about the $\boldsymbol{b}_1$ axis. Spectral stability of this equilibrium, in the special case of a mass-spring damper, is discussed in Ref. 22. Even with damping, however, the symmetries in the system dynamics produce eigenvalues on the imaginary axis. Spectral analysis is therefore inconclusive with regard to nonlinear stability. An attempt was made in Ref. 25 to construct a Lyapunov function for this equilibrium in an approach similar to the energy-Casimir method. Because not all conservation laws were accounted for in the analysis, however, the resulting function was only positive semidefinite; the question of nonlinear stability was not fully resolved.

Recall that, in the special case being considered, the functions

$$C_1 = \boldsymbol{p}_{\mathrm{sys}}\cdot\boldsymbol{p}_{\mathrm{sys}} = \|\boldsymbol{p}_{\mathrm{sys}}\|^2, \qquad C_4 = \boldsymbol{h}_{\mathrm{sys}}\cdot\boldsymbol{p}_{\mathrm{sys}}$$

are Casimirs (see Remark 2.5). If $\boldsymbol{p}_{\mathrm{sys}}$ is initially zero, it remains so for all time. In this case, there exists another conserved quantity called a "subcasimir":

$$C_5 = \boldsymbol{h}_{\mathrm{sys}}\cdot\boldsymbol{h}_{\mathrm{sys}}$$

The gradient of this function is in the null space of $\boldsymbol{\Lambda}$ whenever $C_1 = 0$. More generally, however, this function is not conserved.

When $\boldsymbol{p}_{\mathrm{sys}} = \boldsymbol{0}$, the dimension of the invariant surface (or "leaf") on which the dynamics evolve loses dimension. The equilibrium (28) is called nongeneric because an arbitrarily small perturbation in $\boldsymbol{p}_{\mathrm{sys}}$ raises the dimension of this surface. Here, we will assume that perturbations are restricted to preserve $\boldsymbol{p}_{\mathrm{sys}} = \boldsymbol{0}$. Thus, we will consider "leafwise stability" of the equilibrium (28). To extend conclusions about stability to include perturbations in total linear momentum, one can use the approach described in Ref. 26.

Proposition 3.3: If $J_1 > J_2$ and $J_1 > J_3$, then the equilibrium (28) is leafwise stable if

$$k > \frac{(m_p\Delta)^2}{J_1^2(J_1 - J_3)}\left(h_1^0\right)^2$$

Proof: The equilibrium is a minimum of the Lyapunov function

$$\mathcal{H}_\Phi(z) = \mathcal{H}_U(z) + (1/2M)C_1 - (1/2J_1)C_5$$

where M is any constant satisfying

$$\begin{aligned} \frac{1}{2M} > {} & \left\{ J_1\left(\frac{m_p}{m-m_p}\right)m_p\Delta^2 - \left(J_2 - m_p\Delta^2\right) \right. \\ & \left. \times\left[J_1 - J_2 + \left(\frac{m}{m-m_p}\right)m_p\Delta^2\right]\right\} \Big/ \\ & \left\{(m-m_p)\left[J_2 - \left(\frac{m}{m-m_p}\right)m_p\Delta^2\right] \right. \\ & \left. \times\left[J_1 - J_2 + \left(\frac{m}{m-m_p}\right)m_p\Delta^2\right]\right\} \end{aligned}$$

Nonlinear stability of the equilibrium follows from Lyapunov's direct method. □

Spectral analysis shows that the condition in Proposition 3.3 is sharp in the sense that the equilibrium is unstable if the inequality is reversed. Thus, while steady, major axis rotation is stable with a sufficiently stiff spring mass; this motion becomes unstable when the spring is too weak.

The Lyapunov function in the proof of Proposition 3.3 was constructed using the energy-Casimir method. Unlike the example in Sec. II.D, the stability analysis was more convenient using the Hamiltonian model with a coupled inertia tensor (and a block diagonal Poisson tensor).

IV. Conclusions

Three reduced-dimensional Hamiltonian models were presented for a rigid body interacting with a moving-mass particle. Two cases were considered. In the first, the mass particle was unconstrained. In the second, the mass particle was constrained to move along a linear track fixed within the body. The various Hamiltonian models trade off complexity of the kinetic energy tensor for complexity of the Poisson tensor. Example applications were included to illustrate the utility of these models in analyzing nonlinear stability of steady motions. The first example involved feedback stabilization of steady streamlined descent of a prolate spheroid with a point-mass actuator. Because the feedback control law was based on potential shaping, the closed-loop system remained Hamiltonian. In this example, it was most convenient to use a model with a block-diagonal generalized inertia tensor. The second example involved stability of steady major axis rotation of a spacecraft with a spring-mass oscillator. Conditions on the parameters for nonlinear stability were obtained along with a Lyapunov function proving that the conditions are sufficient. In this example, it was most convenient to use a model with a coupled inertia tensor. To the author's knowledge, this example provides the first proof of Lyapunov stability for the steady motion considered.

In each of the two cases considered, the three models can be shown to be equivalent using recently developed transformation theory for noncanonical Hamiltonian control systems. The existence of equivalent models is valuable for control design and stability analysis. In analyzing nonlinear stability, for example, failure to construct a Lyapunov function for a given steady motion does not imply instability; a choice of Hamiltonian models gives one a greater opportunity to prove stability. The question is how to choose among available Hamiltonian models. Unfortunately, the existing transformation theory provides little guidance. In this paper, the transformations arose from the three most natural representations of the point-mass velocity. For more general systems, it might be valuable to develop guidelines for selecting a transformation based on a particular control design or analysis objective.

Acknowledgments

The author gratefully acknowledges the thoughtful comments and criticisms shared by the anonymous reviewers and by colleagues Chris Hall and Naomi Leonard.

References

[1]Abzug, M. J., "Fuel Slosh in Skewed Tanks," *Journal of Guidance, Control, and Dynamics*, Vol. 19, No. 5, 1996, pp. 1172–1177.

[2]Yam, Y., Mingori, D. L., and Halsmer, D. M., "Stability of a Spinning Axisymmetric Rocket with Dissipative Internal Mass Motion," *Journal of Guidance, Control, and Dynamics*, Vol. 20, No. 2, 1997, pp. 306–312.

[3]Hall, C. D., "Momentum Transfer Dynamics of a Gyrostat with a Discrete Damper," *Journal of Guidance, Control, and Dynamics*, Vol. 20, No. 6, 1997, pp. 1072–1075.

[4]Sandfry, R. A., "Equilibria of a Gyrostat with a Discrete Damper," Ph.D. Dissertation, Dept. of Aerospace and Ocean Engineering, Virginia Polytechnic Inst. and State Univ., Blacksburg, VA, July 2001.

[5]Ross, I. M., "Mechanism for Precision Orbit Control with Applications to Formation Flying," *Journal of Guidance, Control, and Dynamics*, Vol. 25, No. 4, 2002, pp. 818–820.

[6]Shen, J., and McClamroch, N. H., "Translational and Rotational Maneuvers of an Underactuated Space Robot Using Prismatic Actuators," *International Journal of Robotics Research*, Vol. 21, No. 5–6, 2002, pp. 607–618.

[7]Petsopoulos, T., Regan, F. J., and Barlow, J., "Moving-Mass Roll Control System for Fixed-Trim Re-Entry Vehicle," *Journal of Spacecraft and Rockets*, Vol. 33, No. 1, 1996, pp. 54–60.

[8]Robinett, R. D., III, Sturgis, B. R., and Kerr, S. A., "Moving-Mass Roll Control System for Fixed-Trim Re-Entry Vehicle," *Journal of Guidance, Control, and Dynamics*, Vol. 19, No. 5, 1996, pp. 1064–1070.

[9]Woolsey, C. A., and Leonard, N. E., "Stabilizing Underwater Vehicle Motion Using Internal Rotors," *Automatica*, Vol. 38, No. 12, 2002, pp. 2053–2062.

[10]Leonard, N. E., and Graver, J. G., "Model-Based Feedback Control of Autonomous Underwater Gliders," *IEEE Journal of Oceanic Engineering*, Vol. 26, No. 4, 2001, pp. 633–645.

[11]Goldstein, H., *Classical Mechanics*, 2nd ed., Addison Wesley Longman, Reading, MA, 1980, p. 347.

[12]Marsden, J. E., and Ratiu, T. S., *Introduction to Mechanics and Symmetry*. Springer-Verlag, New York, 1994, p. 32.

[13]Blankenstein, G., Ortega, R., and van der Schaft, A., "The Matching Conditions of Controlled Lagrangians and IDA-Passivity Based Control," *International Journal of Control*, Vol. 75, No. 9, 2000, pp. 645–665.

[14]Bloch, A. M., Leonard, N. E., and Marsden, J. E., "Controlled Lagrangians and the Stabilization of Euler–Poincaré Mechanical Systems," *International Journal of Robust and Nonlinear Control*, Vol. 11, No. 3, 2001, pp. 191–214.

[15]Fujimoto, K., and Sugie, T., "Canonical Transformation and Stabilization of Generalized Hamiltonian Systems," *Systems and Control Letters*, Vol. 42, No. 3, 2000, pp. 217–227.

[16]Lamb, H., *Hydrodynamics*, 6th ed., Dover, New York, 1932, Chap. 6.

[17]Newman, J. N., *Marine Hydrodynamics*, MIT Press, Cambridge, MA, 1977, pp. 144–148.

[18]Ostrowski, J. P., "Computing Reduced Equations for Robotic Systems with Constraints and Symmetries," *IEEE Transactions on Robotics and Automation*, Vol. 15, No. 1, 1999, pp. 111–123.

[19]Bloch, A. M., *Nonholonomic Mechanics and Control*, Springer-Verlag, New York, 2003, Chap. 3.

[20]Woolsey, C. A., and Leonard, N. E., "Moving Mass Control for Underwater Vehicles," *Proceedings of the Americal Control Conference*, Vol. 4, American Automatic Control Council, Piscataway, NJ, 2002, pp. 2824–2829.

[21]Leonard, N. E., "Stability of a Bottom-Heavy Underwater Vehicle," *Automatica*, Vol. 33, No. 3, 1997, pp. 331–346.

[22]Hughes, P. C., *Spacecraft Attitude Dynamics*, Wiley, New York, 1986, pp. 61–65.

[23]Woolsey, C. A., "Hamiltonian Attitude Dynamics for a Spacecraft with a Point Mass Oscillator," *Electronic Proceedings of the 15th International Symposium on Mathematical Theory of Networks and Systems*, edited by D. S. Gilliam and J. Rosenthal, Univ. of Notre Dame, South Bend, IN, 2002.

[24]Chinnery, A. E., and Hall, C. D., "Motion of a Rigid Body with an Attached Spring-Mass Damper," *Journal of Guidance, Control, and Dynamics*, Vol. 18, No. 6, 1995, pp. 1404–1409.

[25]Chinnery, A. E., "Numerical Analysis of the Motion of a Rigid Body with an Attached Spring-Mass-Damper," M.S. Thesis, Dept. of Aerospace and Systems Engineering, Air Force Inst. of Technology, Wright–Patterson AFB, OH, Dec. 1993.

[26]Leonard, N. E., and Marsden, J. E., "Stability and Drift of Underwater Vehicle Dynamics: Mechanical Systems with Rigid Motion Symmetry," *Physica D*, Vol. 105, June 1997, pp. 130–162.